

## Interferometric Studies of Faster than Sound Phenomena. Part II. Analysis of Supersonic Air Jets\*

R. LADENBURG, C. C. VAN VOORHIS, AND J. WINCKLER

*Palmer Physical Laboratory, Princeton University, Princeton, New Jersey*

(Received April 4, 1949)

A study of supersonic air jets has been made by the use of the Mach interferometer. The density distribution in axially symmetric jets with several tank-receiver pressure ratios has been determined, with special emphasis on the 3.7-7 range of ratios. In terms of the dimensionless quantities  $\rho/\rho_0$  (ratio of jet density to tank density) and  $Z/D$  (ratio of distance from orifice to orifice diameter), all jets are closely the same in a region bounded by the orifice and an oblique line from the orifice edge. This line marks an inflection point in the streamlines, and probably indicates the low pressure termination of a three-dimensional Prandtl-Meyer expansion region which reduces the pressure at this point below that of the receiver. The strength of the stationary shock wave in general agrees with that predicted by the Rankine-Hugoniot equations. Recent theoretical computations of the density in the axis of the jets by Owen and Thornhill are in satisfactory agreement with the experimental results, but so far no suggestion has appeared for a theory to predict the three-shock configuration in jets.

Experiments with two-dimensional jets confined between parallel glass walls demonstrated that the *stationary* three-shock configuration could not be studied in this way, presumably because of boundary layer effects on the glass which destroy the two-dimensional quality of strong shock waves.

### I. INTRODUCTION

THE study of the flow of gases from a reservoir through an orifice into a receiver dates back to the original work of St. Venant and Wantzel<sup>1</sup> more than a century ago. The existing knowledge of the compressible flow of gases through pipes and orifices is summarized in most textbooks on gas dynamics.<sup>2</sup>

A significant advance was made by Osborne Reynolds,<sup>3</sup> who discovered in 1885 that, if the ratio of the receiver to reservoir pressure drops below a certain critical value  $P/P_0 = [2/(\gamma+1)]^{\gamma/(\gamma-1)}$ , the velocity of the gas at the narrowest part of the passage reaches the local velocity of sound, but up to the point of reaching the constriction, the flow is unaffected by the receiver conditions. If the pressure ratio  $P/P_0$  is lower than the critical value, the jet expands into the receiver, attaining supersonic velocity. In such supersonic jets stationary patterns, consisting of expansions and constrictions accompanied by shock waves,<sup>4</sup> appear, under certain conditions repeating themselves many times as the jet proceeds out from the orifice.

Since this is the most prominent feature of such jets, it was the first to be studied by various authors, originally by E. Mach and Salcher,<sup>4</sup> later by Emden,<sup>5</sup> and

Prandtl,<sup>6,7</sup> by means of the schlieren and shadowgraph technique, and recently by Hartmann and Lazarus.<sup>8</sup> Theoretical explanations for the periodic structure were given by Prandtl,<sup>7</sup> von Karman,<sup>9</sup> and Lord Rayleigh.<sup>10</sup> An account of the mathematical ideas involved (especially those of Rayleigh) and a bibliography on the subject are given by Bateman.<sup>2</sup> Such derivations assume that the gas velocity normal to the jet direction is small, or, in other words, that the jet expands very little, its pressure being about the same as the receiver, and that conditions throughout the jet are nearly constant. The adiabatic law, or the existence of a velocity potential is also assumed throughout the flow. Under these assumptions a wave-length,  $\lambda$ , representing the distance between the successive "disks" or periods of expansion and contraction as shown in Mach's and Emden's photographs, is obtained, in more or less agreement with some of the experiments. These derivations are certainly not applicable when the jet undergoes an appreciable radial expansion. Also, the existence of standing discontinuities which make the flow non-isentropic, and the turbulent mixing of the jet stream with the surrounding air, along with the other effects of viscosity and heat conduction, are neglected in these treatments.

It is evident that more knowledge, both theoretical and experimental, must be forthcoming before a general treatment, which holds over a wide range of pressure and expansion ratios, can be made.

The proper approach to the subject would seem to be to study in detail the structure of only the first section, or period, and such is the purpose of this paper. L.

\* The present work as well as that described in Part I (Phys. Rev. **73**, 1358 (1948)) was done under Contract NORD 9240 with the Bureau of Ordnance, Navy Department.

<sup>1</sup> B. De Saint-Venant and L. Wantzel, J. de l'Ecole Polytechnique **16**, 85 (1839).

<sup>2</sup> See, for example, J. Ackeret, *Handbuch der Physik* (Verlag. Julius Springer, Berlin, 1927), Vol. 7, Chapter 5; H. Bateman, Committee on Hydrodynamics, Part 4: "Compressible fluids" (Bull. Nat. Res. Council, No. 84, February 1932); G. I. Taylor and J. W. Maccoll, *Aerodynamic Theory* (Verlag. Julius Springer, Berlin, 1935), edited by W. F. Durand, Vol. 3, Division H.

<sup>3</sup> Osborne Reynolds, Phil. Mag. **21**, 185-199 (1886).

<sup>4</sup> The shocks, or sudden discontinuities in the density, pressure, temperature, and velocity of the air in the jet are fundamentally the same as those arising from an explosion.

<sup>5</sup> E. Mach and P. Salcher, Wien. Ber. **98**, 1303-1309 (1889).

<sup>6</sup> R. Emden, Ann. d. Physik **69**, 264-269, 426-455 (1899).

<sup>7</sup> L. Prandtl, Physik. Zeits. **5**, 599-601 (1904). See also his book, *Strömungslehre* (Friedrich Vieweg & Sohn, Braunschweig, 1944), second edition, Abschnitt II.

<sup>8</sup> L. Prandtl, Physik. Zeits. **8**, 23-30 (1907); E. Magin, Forschungsheft Ingenieurwesen **62**, 1-32 (1908).

<sup>9</sup> J. Hartmann and F. Lazarus, Phil. Mag. **31**, 35-50 (1941).

<sup>10</sup> Th. von Karman, Physik. Zeits. **8**, 209-211 (1907).

<sup>11</sup> Lord Rayleigh, Phil. Mag. **6**, 177-187 (1916).

Mach<sup>11</sup> made such a study in some detail qualitatively, using schlieren and interferometric techniques for the optical examination. He showed that standing "sound" waves of conical shape (called *schiefer Verdichtungsstoss* in German literature), similar to those observed ahead of a projectile in flight, existed in the jet, and that these waves could be reflected at the free boundary between the jet and the atmosphere due to the sudden change in velocity of the gas at this point. Furthermore, at low reservoir pressure he showed that these conical "sound" waves intersected in a simple way to form an X, but at higher pressures they become stronger and a flat shock wave normal to the stream appeared (called *gerader Verdichtungsstoss*). This he interpreted to be the same kind of interaction as observed and studied in detail earlier by E. Mach<sup>12</sup> when two explosion waves collided, or when an explosion wave was reflected from a surface.<sup>b</sup> L. Mach also found from a rough quantitative evaluation of the interference photographs that the air density in the jet at emergence was, in general, higher than that of the atmosphere, but that at distances out from the orifice the density dropped far below atmospheric density in many cases.

Cranz and Glatzel<sup>13</sup> made a study of jets at very high pressures formed by the ejection of powder gases from an 8-mm gun. They measured the Mach number distribution with probes and made shadowgrams of the

shock formations. It has been shown in connection with the present work that these velocity measurements are in error, however, due to boundary layer phenomena.<sup>c</sup> W. Pupp, working in Cranz's laboratory, made what is probably the first quantitative evaluation of the density in a supersonic jet by interferometry. This is described in Cranz's *Ballistik* (Vol. II, p. 192), but in insufficient detail for comparison with the present study, as only axial pressure values are given.

Stanton<sup>14</sup> investigated certain properties of jets, particularly the conditions just at the orifice, by using static pressure probes and pitot tubes. He determined the exact position of the minimum cross section, the effect of scaling, and measured the pressure distribution along the axis of the jet. His results are not complete enough to determine the flow pattern and shock wave formation of the jet, however. His values of  $P/P_0$  were in the vicinity of the critical value.

Hartmann and Lazarus<sup>8</sup> explored the pressure distribution along the axis of jets at reservoir pressures up to 7 kg/cm<sup>2</sup> using a pitot tube. Axial pressure curves were obtained in jets exhibiting both the simple X and the more complex shock interaction observed by Mach. The pitot measurements were in agreement with measurements of the Mach number using probes, in the case of the simple X interaction. These measurements constitute the best quantitative data we have found so far for supersonic jets, but are not complete as only the axial region is explored. The schlieren photos made by Hartmann and Lazarus are valuable for qualitative examination.

Prandtl<sup>7</sup> was the first to interpret the formation of a free jet by determining what shape and direction a very weak shock wave, or sound wave ("Mach line"), would

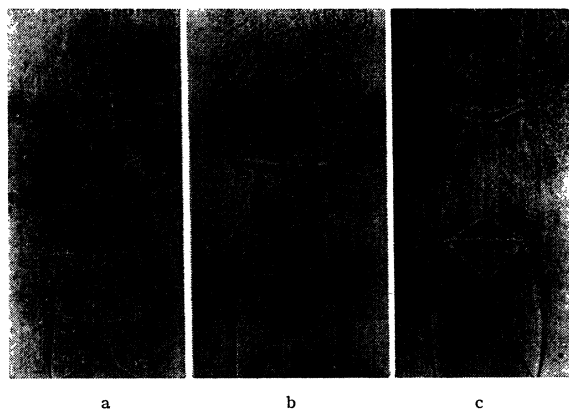


FIG. 1A. Shadowgrams of axially symmetric air jets flowing upward from a round orifice of 10-mm diameter. The black lines are generally the outlines of standing shock wave formations. The tank gauge pressure in a, b, and c are 20, 30, and 40 lb./in.<sup>2</sup>, respectively.

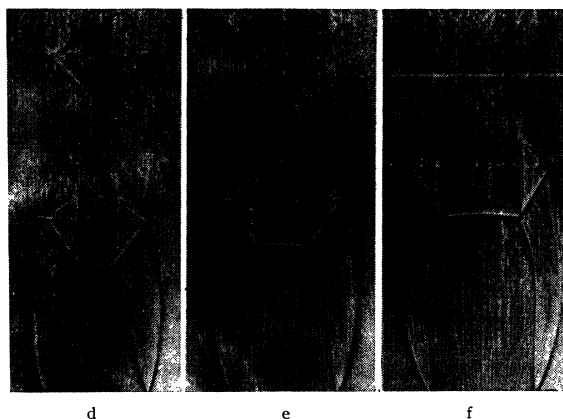


FIG. 1B. Shadowgrams as in Fig. 1A, the tank gauge pressures in d, e, and f are 60, 80, and 110 lb./in.<sup>2</sup>, respectively.

<sup>11</sup> L. Mach, Wien. Ber. 106-II, 1025-1074 (1897).  
<sup>12</sup> E. Mach and J. Wosyka, Wien. Ber. 72-II, 44-50 (1875). W. Rosicky, Wien. Ber. 73-II, 629-650 (1876). E. Mach and J. Sommer, Wien. Ber. 75-II, 101-130 (1877). Mach, Tumlriz, and Kogler, Wien. Ber. 77-II, 7-32 (1878). E. Mach, Wien. Ber. 77-II, 819-838 (1878). E. Mach and G. Gruss, Wien. Ber. 78-II, 467-480 (1878). E. Mach and J. Simonides, Wien. Ber. 80-II, 476-486 (1879). E. Mach and L. Mach, Wien. Ber. 98-II, 1333-1336 (1889).  
<sup>b</sup> The importance of E. Mach's discovery of such "triple shocks" to modern studies of shock waves and their interaction, was pointed out by J. von Neumann, R. J. Seeger, and others (reference 15).  
<sup>13</sup> C. Cranz and B. Glatzel, Ann. d. Physik 43, 1186 (1914).

<sup>c</sup> In regions where strong standing shock waves exist, the boundary layers along the probes used for the measurements of Mach numbers suffer separation and lead to diversion of the flow. Details of these disturbing effects are published in Part III of our interferometric studies NAVORD Report 7-47. See also Fig. 13 of reference 16b.  
<sup>14</sup> T. E. Stanton, Proc. Roy. Soc. 111-A, 306 (1926).

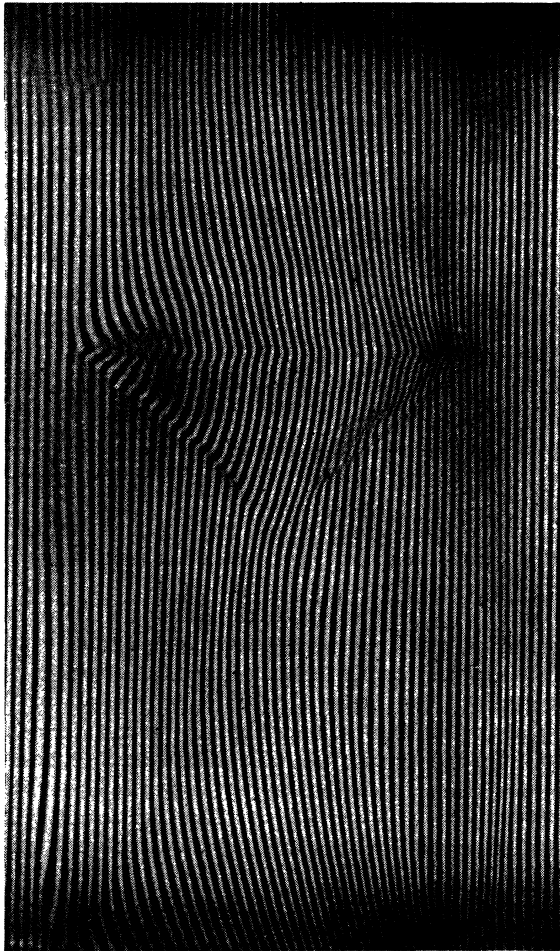


FIG. 2. Interferogram of an air jet issuing upward from a tank at 40-lb./in.<sup>2</sup> gauge through a 10-mm-diameter round orifice. (Compare with the shadowgram *c* of Fig. 1A.) The exposure ( $\sim 300 \mu\text{sec}$ .) was too long to show turbulence.

assume at various parts of the jet. He showed that the wedge-shaped expansion region which arises from the orifice edge as the gas stream turns outward into the atmosphere (see especially his Figs. 7 and 9), is reflected from the opposite free boundary of the jet with a change of phase, and proceeds onward as a compression region, is again reflected as an expansion region, and so on, producing the periodic structure of the jet. Prandtl does not discuss the shock formations observed by Mach in jets.<sup>11, 15</sup>

The present investigations as well as two others<sup>16, 17</sup>

<sup>15</sup> Seeger, von Neumann, and Polachek, *Phys. Rev.* **69**, 677 (1946); H. Polachek and R. J. Seeger, *Phys. Rev.* **69**, 677; L. G. Smith, *Phys. Rev.* **69**, 678; A. H. Taub and L. G. Smith, *Phys. Rev.* **69**, 678. See also H. W. Liepmann and A. E. Puckett, *Introduction to Aerodynamics of a Compressible Fluid*, GALCIT Aeronautical Series (John Wiley & Sons, Inc., New York, 1947), p. 60.

<sup>16</sup> (a) Ladenburg, Van Voorhis, and Winckler, NAVORD Report 69-46 (Navy Bureau of Ordnance publication). (b) J. R. Winckler, *Rev. Sci. Inst.* **19**, 307 (1948).

<sup>17</sup> Ladenburg, Winckler, and Van Voorhis, *Phys. Rev.* **73**, 1372 (1948).

originated during the war when the senior author (R. L.) studied at the Ballistic Research Laboratory of Aberdeen Proving Ground the behavior of powder gases ejected from guns in connection with the formation and elimination of gun flash. When it became clear that the typical shocks in the ejected gases, through the increase of pressure and temperature, were essential for the gun flash, at least for the "primary" flash, the interferometric method was suggested for the quantitative study of the physical conditions of jets, since this method had been used extensively by R. L. for the investigation of the dispersion, especially the "anomalous" dispersion of gases (see *Rev. Mod. Phys.* **5**, 248, 1933). The experiments described in this paper were carried out in the years 1945 and 1946.

## II. DESCRIPTION OF EXPERIMENTS

### A. Axially Symmetric Jets at Pressure Ratios from 2:1 to 8:1

The techniques developed by the writers and described elsewhere (references 16, 17) have been used in studying axially symmetric air jets over a wide range of pressure ratios. In these experiments dry air from a pressure tank discharged through a valve and a cylin-

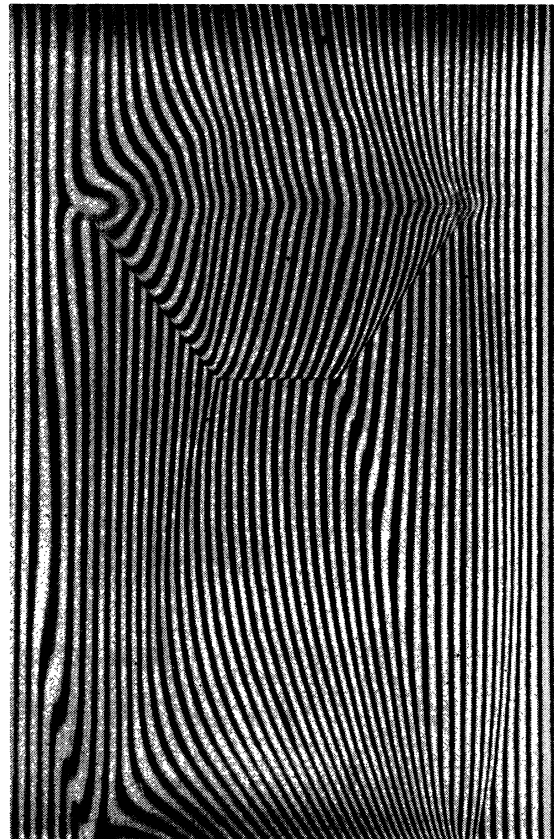


FIG. 3. Interferogram of an air jet at 60-lb./in.<sup>2</sup> gauge tank pressure (compare with shadowgram *d* of Fig. 1B). Exposure  $\sim 300 \mu\text{sec}$ .

dricul tube with a streamlined orifice into the open atmosphere, forming an air jet. The orifice was placed in one light beam of a Mach interferometer (see Fig. 9; also Figs. 2 and 10 of reference 16b). The valve was either opened quickly by hand and a spark as light source flashed by an automatic switch when the tank pressure dropped to a predetermined value, or the valve was opened to synchronize with a rotating shutter when using a mercury arc. This instrumentation has been used without modification to study jets at various tank pressures between 20 and 100 lb./in.<sup>2</sup> gauge, or a tank ÷ room pressure ratio of about 8 maximum. Some experiments were carried out with a modified orifice having a much more gradual constricting section than that described in reference 16b, Fig. 10, but the geometrical shape of the jet and of the shock formations did not change appreciably. To extend the ratio to higher values, the jet was discharged into a vacuum chamber equipped with nearly plane-parallel windows (see Part II-B). Some measurements were also attempted with a two-dimensional jet confined between such windows.

The characteristic features of such air jets are shown qualitatively by shadowgrams (Figs. 1A and 1B, made with a fast light source of about 10  $\mu$ sec. duration (mercury arc)). Any discontinuities in density, such as shock waves and slip streams, appear as dark and light bands. The interesting feature is the development of the shock wave formation, which up to nearly 40 lb. pressure is conical. At greater pressures, a normal shock appears, accompanied by a slip stream extending upward from the three-shock intersection. The air emerges upward from a round orifice constricted smoothly from the valve opening (25 mm) to the orifice diameter (10 mm). (For details, see reference 16). It seems, according to these shadowgrams, as if a continuous shock starts at the edge of the orifice and extends up to the edge of the normal shock. But this is actually not so. As will be explained in more detail in Section III, the apparently continuous line consists of a density "valley" extending up from the orifice, joining in some cases to a shock wave which forms farther up in the jet. The "valley" has an optical effect in schlieren and shadow photographs identical with a shock wave. The difference is shown only by interferometer photographs and analysis.

Figures 2, 3, and 4 are interferograms of air jets at 40, 60, and 80 lb./in.<sup>2</sup>, respectively, and are typical of the jets studied. The unsymmetrical appearance of the fringes is due to the fact that a density decrease, for example, moves the fringes perpendicular to themselves always in the same direction, therefore they crowd on one side of the axis and expand at a symmetrical point on the other side of the axis, although the change of density is the same at symmetrical points. In addition, interferograms were also made and analyzed at 20, 30, and 100 lb./in.<sup>2</sup>. An interferogram of a 60-lb./in.<sup>2</sup> jet emerging from a 4-mm diameter orifice similar to the

10-mm was also analyzed. The shock waves are revealed by sudden displacements of the fringes and are seen to correspond in position to the light and dark bands shown in the shadowgrams. One sees also that many portions of the jets, especially at 80 lb./in.<sup>2</sup> pressure, are very turbulent as shown by irregular variations in the fringes. This effect is probably in the boundary which surrounds the entire jet. The narrow horizontal sections in Fig. 4 contain undisplaced fringes for reference, which are superposed photographically on the main part of the interferogram by two sets of grids.

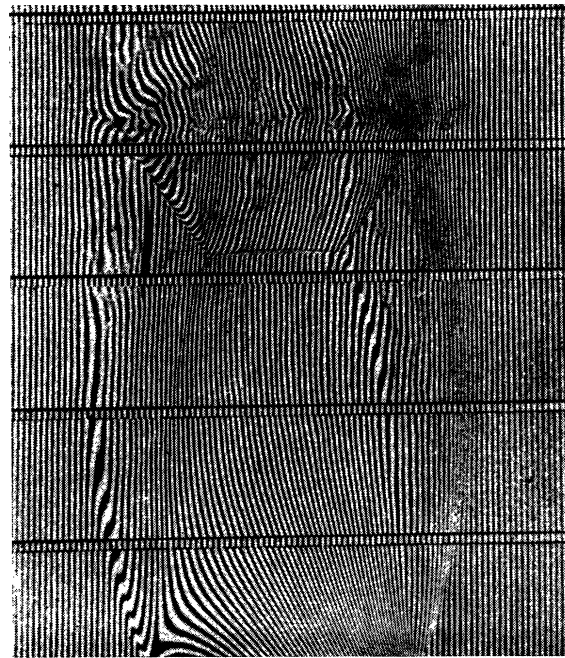


FIG. 4. Interferogram of an air jet at 80-lb./in.<sup>2</sup> gauge tank pressure (compare with shadowgram *e* of Fig. 1A.) Undisplaced fringes are superimposed in the narrow bands by means of grids. Note the turbulence, probably in the jet boundary, shown by irregularities in the fringes. Exposure 1  $\mu$ sec.

Figures 2 and 3 were photographed with a powerful mercury arc and fast shutter ( $\sim 300 \mu$ sec.), while for Fig. 4 an air spark of only 1- $\mu$ sec. duration between magnesium electrodes was used. (Light sources are described in reference 16.)

The interferograms obtained on spectroscopic plates were measured with great care on a comparator with accurate scales in two perpendicular directions. Between 20 and 30 separate cross sections were measured and evaluated on each interferogram, spaced very close together in the triple-shock intersection region, and wider elsewhere. The fringe shifts were calculated and plotted in the usual way, using the scheme described in reference 16, averages being taken of the two symmetrical halves of each section. Reduction of fringe shift values to densities was carried out at the Navy Department, Bureau of Ordnance, in accordance with a

mechanized scheme developed for axially symmetric flows. This procedure is described in reference 17, and has replaced the slower methods discussed in reference 16 for this phase of the reduction.

The density contours resulting from an analysis of the 40-, 60-, and 80-lb. jets are given, respectively, in Figs. 5, 6, and 7.<sup>d</sup> The numbers on the charts are in  $\text{mg}/\text{cm}^3$ . A glance at these charts and at the shadowgrams of Figs. 1A and 1B indicates that the analysis has preserved the shock contours reasonably well. One observes that the density drops rapidly from its value at the orifice as the air expands into the jet.

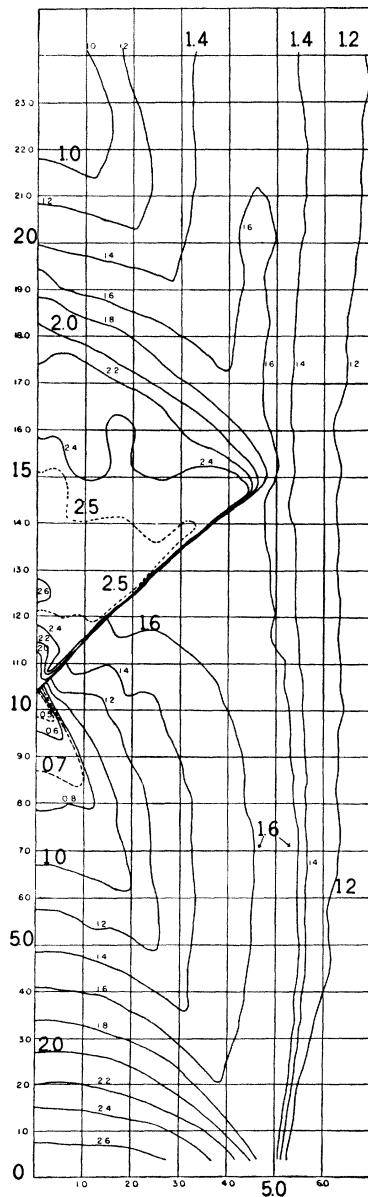


FIG. 5. Density contours for an axially symmetric supersonic air jet. Tank gauge pressure 40 lb./in.<sup>2</sup> (compare shadowgram *c* of Fig. 1A and interferogram Fig. 2). The isopycnic lines are labeled in units of  $\text{mg}/\text{cm}^3$ . Corresponding values of pressure etc. are given in Table I.

<sup>d</sup> Complete sets of large-sized density charts and original photographs of all jets analyzed are being prepared in a limited quantity by Palmer Physical Laboratory and will be available to specially interested persons.

There is a sudden, apparently discontinuous increase across the various shock fronts, and a gradual transition to normal density at the jet boundary. If one is willing to assume an isentropic expansion of the air from the pressure tank up to regions in the jet bounded by the orifice, the turbulent boundary and the shock waves, then the pressure, temperature, and velocity may be calculated from well-known hydrodynamical relations since the stagnation pressure  $P_0$ , temperature  $T_0$  and density  $\rho_0$  are known. Tables I, II, and III have been prepared using these relations, with the various constants applying to the 40-, 60-, and 80-lb. jets, and enable one to obtain the pressure and other variables directly from the jet density within the region bounded by the orifice, the turbulent boundary and the shock waves. The additional application of the Rankine-Hugoniot relations permits one to determine changes in these variables across shocks, where the flow is not isentropic.<sup>e</sup> Especially remarkable are the deep minima in the isopycnic curves which mark also regions of minimum pressure, the line connecting these minima will be designated as "valley" in the following discussions in Section III.

### B. Axially Symmetric Jets at Pressure Ratios up to 200:1

The 1.5-m<sup>3</sup> tank used primarily for the jet studies had a maximum working pressure of 100 lb./in.<sup>2</sup>, which provided a jet discharging into the atmosphere at a pressure ratio of about eight. To increase the pressure ratio, a vacuum tank was added to the system, and the jet was discharged into a chamber at various degrees of evacuation. The chamber was located in one beam of the interferometer, and light was admitted through glass windows of the best optical quality. Compensating glass plates were added to the other interferometer beam. A sketch of the arrangement is shown in Fig. 8, and Fig. 9 gives a photographic view of the actual apparatus. The vacuum chamber is a circular tube of 10-cm inside diameter, which is connected by a 90° elbow and a siphon bellows to a vacuum tank of about  $\frac{3}{4}$ -m<sup>3</sup> capacity. The orifice, valve and pressure tank are the same as before.

Face plates containing openings were welded to the sides of the tube, and their surfaces were carefully ground. The window glasses are held against these face plates directly and sealed from the side with rubber gaskets. The compensating chamber is a tube in a horizontal position, also with ground end plates against which the compensating windows are held. The vacuum chamber window glasses are 2 in.  $\times$  4 in., while those on the compensating chamber are 2 in.  $\times$  2 in. All four plates were cut from a plane disk of 7½-in. diameter and ½-in. thickness, which had a wedge error of about two wave-lengths. The wedge error was compensated by mounting the windows in a reverse position to that originally occupied in

<sup>e</sup> For a derivation of these relations see textbooks such as Liepmann and Puckett, *Introduction to the Aerodynamics of a Compressible Fluid* (John Wiley & Sons, Inc., New York, 1947); or R. Sauer, *Theoretische Einführung in die Gasdynamik* (Verlag. Julius Springer, Berlin, 1943), English translation published by Edwards Brothers, Ann Arbor.

the circular plate. The result was that the introduction of the vacuum chamber and compensating chamber into the interferometer produced no perceptible distortion of the interference fringes.

The chamber could be raised or lowered by a telescoping section, with a number of cylindrical spacer rings equal in diameter to the inner tube. The inside wall surface between tank and orifice was thus kept smooth, while utilizing the full area of the 4-in. high window with the 1-in. high field of view of the interferometer.

The camera consisted simply of a 3-in. diameter, 60-cm lens of good quality, a mirror to reduce the space needed, and a plate holder. Images of the interference fringes at the jet were produced in exactly natural size on the photographic plate.

The vacuum chamber was not suited to shadow photography as the photographic plate could not be brought near to the jet, and also because the low air density gave very weak effects. Schlieren studies were made by turning the vacuum chamber by 90°, which, on removal of the compensating chamber, provided a clear path for light between the interferometer mirror supports. Two schlieren lenses, a knife edge and a suitable camera objective were used in the conventional manner.

The pressure in the vacuum chamber was determined by a calibrated vacuum gauge connected to a manifold with four tubes leading to four points near the bottom of the chamber. The compensating chamber was ordinarily kept at atmospheric pressure.

The temperature within the vacuum chamber was in general lower than normal due to cooling by the expanding gas of the jet. The density, which had to be known in the region outside the jet proper for interpreting the interferograms, could therefore not be calculated from the pressure alone. The density was determined by moving film records made with a General Radio Recording Camera (see reference 16). A known vacuum was produced in the chamber, the camera was started, and the jet produced by opening the valve. The shift  $\Delta s$  of the fringes from the known initial condition could be determined, and the density  $\rho'$  in the homogeneous region outside the jet calculated, using the known length  $d$  of the light path, through the chamber, from the relation  $\rho' = \rho_0 + \Delta s \lambda / K d$ .  $K$  is the Gladstone-Dale factor,  $\lambda$  the light wavelength and  $\rho_0$  the density of air in the other interferometer beam.

The 4-mm streamlined orifice mentioned in Section II-A was used in the vacuum chamber, as the smaller size permitted the observation of larger expansions without exceeding the limits of the field of view.

Interferograms were made and reduced in the usual manner for cases of axial symmetry.

In Fig. 10 a series of schlieren photographs of jets at various expansion ratios is presented. The knife edge was perpendicular to the flow, with the result that the jet appears symmetrical, but shows the large  $Z$ -gradient near the orifice. At the higher ratio the density drops to so low a value near the shock region that the optical effect is quite small. The sharpness and contrast of the shocks decrease at higher expansion ratio, as the overall density and consequently the optical effect is smaller.

Figure 11A is an interferogram of a jet at an expansion ratio of 210. Due to its large extension, two sections obtained by changing the height of the chamber have been fitted together. Figure 11A, as well as 11B and 11C, were made with an initial adjustment of the interferometer so that one fringe covered the entire field, i.e., so that the field had a uniform color. Fringes then appear if the density is not uniform when the jet is turned on. Each fringe represents a line of constant integrated density through the jet. Such interferograms can be

interpreted directly in two-dimensional flow, but for axial symmetry they give qualitative results only. This will be known, henceforth, as the method of *fringe contours*.

In Figures 11B and 11C the jet expanded at a ratio of

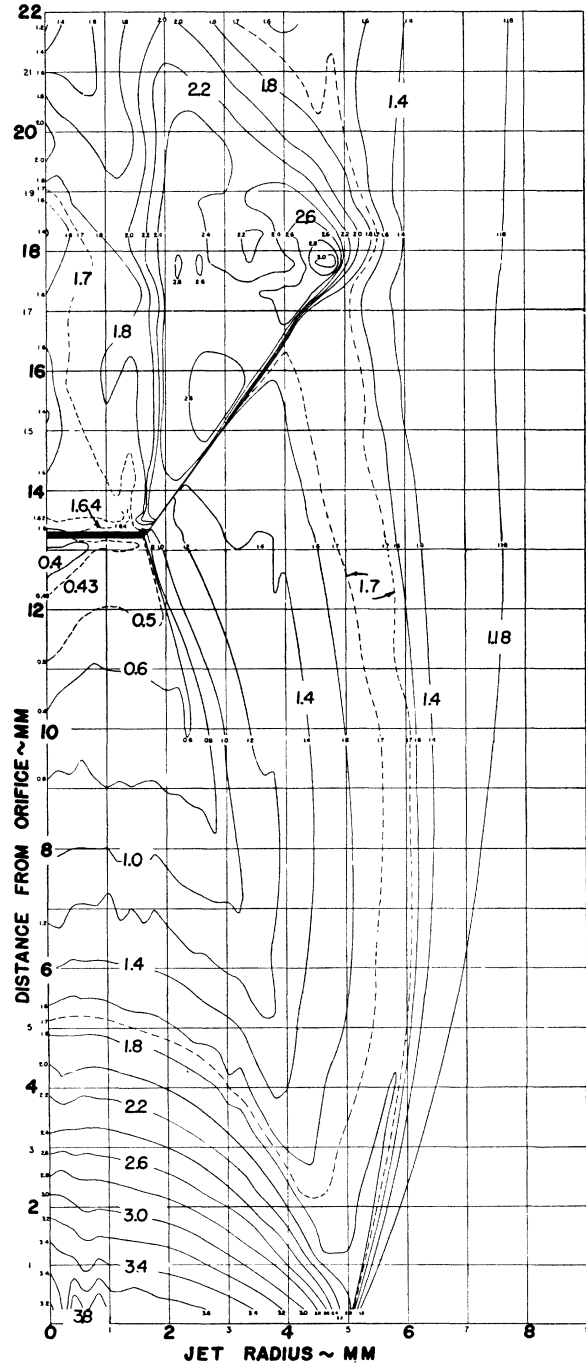


Fig. 6. Density contours for an axially symmetric supersonic air jet at a tank gauge pressure of 60 lb./in.<sup>2</sup> (compare shadowgram  $d$  of Fig. 1B and interferogram Fig. 3). The isopycnic lines are labeled in units of mg/cm<sup>3</sup>. Corresponding values of pressure etc. below the strong normal shock are given in Table II.

nearly 60, but the tank pressure in 11C was 17.7 lb./in.<sup>2</sup> gauge whereas it was 103 lb./in.<sup>2</sup> in 11B.

Figure 12 is an interferogram at ratio 60 with the field initially filled with straight vertical fringes. This interferogram has been completely analyzed in the usual manner, but the isopycnal chart is not reproduced here; due to the very low density, the relative accuracy is poor especially at points near the shock region. In fact, the analysis yielded negative density values in the region near the axis, probably due to the turbulence at the boundary between jet and surrounding air or some asymmetry in the jet.

### III. INTERPRETATION OF EXPERIMENTAL RESULTS

From the isopycnal charts of jets at various pressures (Figs. 5, 6, and 7) as well as from shadowgrams (Fig. 1) and schlieren photographs (Fig. 10), it is seen that there is a regular dependence of jet structure on tank pressure. The jet progressively enlarges, accompanied by a

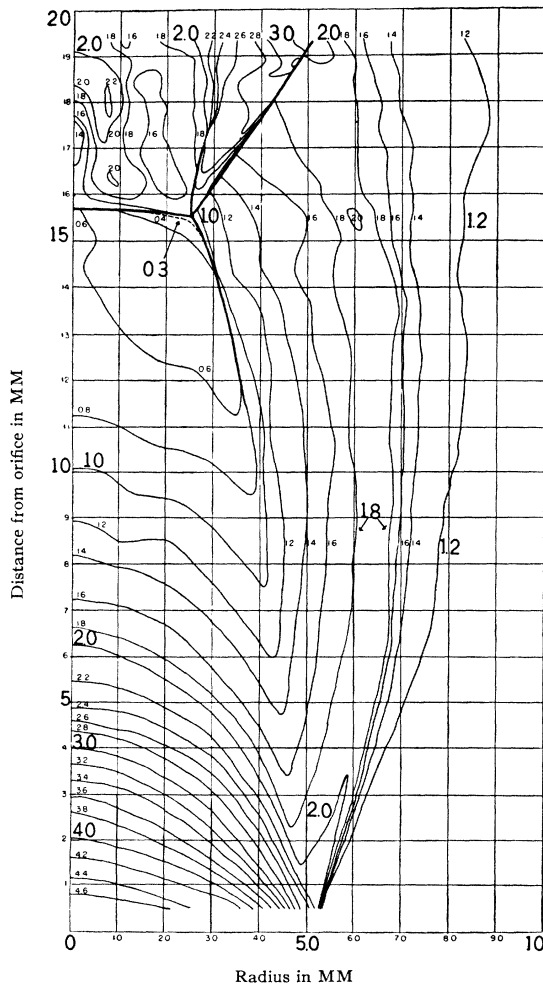


FIG. 7. Density contours for an axially symmetric supersonic air jet at a tank gauge pressure of 80 lb./in.<sup>2</sup> (compare shadowgram  $\sigma$  of Fig. 1B and interferogram Fig. 4). The isopycnal lines are labeled in units of mg/cm<sup>3</sup>. Corresponding values of pressure etc. below the strong normal shock are given in Table III.

characteristic system of stationary shock waves, which at low ratios appear on the photographs as oblique lines crossing at the jet center. At higher ratios the shocks appear much stronger and a normal shock appears in the central part of the jet, accompanied by a slip stream extending downstream from the intersection point of the three shocks.

For the interpretation of the structure of the various jets the following ideas are helpful:

(A) The assumption of isentropic flow from the tank through the valve and orifice and out into the jet, up to the point where shock waves occur;

(B) the fact that most features of the jets are functions of the dimensionless quantity  $\rho/\rho_0$ , where  $\rho$  is the density of points in the jet and  $\rho_0$  is the tank density;

(C) the assumption of a Prandtl-Meyer expansion region at the edge of the orifice, where the jet expands into the lower pressure region of the receiver;

(D) the applicability of the Rankine-Hugoniot relations to all shock waves in the jets;

(E) the possibility of applying to the jet shocks the shock wave theory for the reflexion of shocks in ideal gases as developed by von Neumann, Polachek and Seeger (reference 15);

(F) the construction of streamlines and Mach lines computed by the numerical-graphical integration of the general flow equations.

Some of these ideas are discussed also by Pack in a recent paper,<sup>18</sup> where he computes the formation of shock waves in jets for two-dimensional flow.

Let us now consider the various points.

#### A. The Assumption of Isentropic Flow

This assumption has been used in calculating pressure, temperature, Mach number and velocity, for example in the Tables I, II, and III; the well known equations are given in Table I. The Mach number values were checked experimentally by probes in several instances, and good agreement was found except in the boundary layer, where turbulence and mixing occur, and some distance upstream of the strong normal shock.<sup>1</sup> Changes of entropy occur across shock waves, so the above assumption holds in the jets only between orifice and shock wave region.

#### B. Dependence of Most Features of Jets on $\rho/\rho_0$

If one plots  $\rho/\rho_0$  as a function of the ratio  $Z/D$  with  $R/D$  constant, where  $Z$  is the distance from the jet orifice,  $D$  the jet diameter and  $R$  the distance from the jet axis, it is found that all jets fall on one curve,<sup>2</sup> and depart therefrom at a definite value of  $Z$  depending

<sup>18</sup> D. C. Pack, *Quart. J. of Mech. and App. Math.* **1**, Part 1, (1948).

<sup>1</sup> Details of these disturbing effects are published in Part III of our interferometric studies NAVORD Report 7-47.

<sup>2</sup> The theoretical justification for this "scaling" is given, for example, in the recent paper by Pack (reference 18).

TABLE I. Pressure, etc., as adiabatic functions of density (40-lb./in.<sup>2</sup> jet).  $P/P_0=(\rho/\rho_0)^\gamma$ ;  $T/T_0=(\rho/\rho_0)^{\gamma-1}$ ;  $M^2=V^2/a^2=2(T_0-T)/T(\gamma-1)$ ;  $V^2=2C_p(T_0-T)$ ;  $\gamma=C_p/C_v=1.404$ ;  $C_p=1.00 \times 10^7$  erg/g °K;  $\rho_0=4.41$  mg/cm<sup>3</sup>;  $P_0=3.74$  atmos.;  $T_0=298^\circ\text{K}$ .

Density $\rho$ (mg/cm <sup>3</sup> )	Pressure $P$ (atmos.)	Temperature $T$ (°K)	Mach No. $M$	Velocity $V$ (meter/sec.)
0.2	0.05	85	3.51	652
0.3	0.08	101	3.12	628
0.4	0.13	113	2.85	607
0.6	0.22	133	2.48	573
0.8	0.34	149	2.21	545
1.0	0.46	163	2.03	520
1.2	0.60	175	1.85	494
1.4	0.74	186	1.71	472
1.6	0.89	196	1.58	450
1.8	1.05	206	1.47	428
2.0	1.22	216	1.36	405
2.2	1.39	224	1.27	385
2.4	1.57	232	1.18	364
2.6	1.76	239	1.09	344
2.8	1.95	246	1.00	322

on the reservoir pressure. This value of  $Z$  corresponds to a shock wave or compression region. Figure 13 is a typical example of such a curve compounded from the isopycnal charts of all jets analyzed except the jet at the expansion ratio 60.

The plotted points are the values of  $\rho/\rho_0$  on a line at  $R/D=0.1$  parallel to the axis. It is seen that the experimental points for various jets group closely around the mean curve, up to the point where a shock or compression occurs in each case (see Section III-D below). Similar curves were drawn in addition at values of  $R/D=0.0, 0.2, 0.3, 0.4,$  and  $0.45,$  all of which behave in a way similar to Fig. 13. From this set of curves a new composite chart representing all jets at once was constructed (Fig. 14). The contours represent points of constancy of the ratio  $\rho/\rho_0$ . The figure shows that this ratio and all values such as pressure, temperature, Mach numbers, etc., dependent on it, are identical in the various jets in a region bounded by the orifice and a line (dotted in Fig. 14) drawn from the orifice edge through the minima in the isopycnal charts. This is the "valley" mentioned at the end of Section II-A. These lines either meet the jet axis some distance from the orifice or they meet the triple-shock intersection away from the axis. In the latter case the line of the normal shock wave closes the region. Values of pressure ratio  $P/P_0=(\rho/\rho_0)^\gamma$  are given in Fig. 14 on each contour, as well as the geometrical shape and location of the shock formations for the 40-, 60-, 80-, and 100-lb./in.<sup>2</sup> jets. It is to be understood that the over-all figure is for the 100-lb./in.<sup>2</sup> jet, but that this represents also the other pressures up to the position of the dotted line referred to above.

These considerations and conclusions have been confirmed recently to some extent by a paper by Owen and Thornhill of the Armament Research Establishment, British Ministry of Supply,<sup>19</sup> who calculated by the

<sup>19</sup> P. L. Owen and C. K. Thornhill, A. R. E. Report No. 30/48, Fort Halstead, Kent (September 1948).

Table II. Pressure, etc., as adiabatic functions of density (60-lb./in.<sup>2</sup> jet). (For equations used, see Table I.)  $C_p=1.00 \times 10^7$  erg/g °K;  $\rho_0=6.06$  mg/cm<sup>3</sup>;  $P_0=5.08$  atmos.;  $T_0=297^\circ\text{K}$ .

Density $\rho$ (mg/cm <sup>3</sup> )	Pressure $P$ (atmos.)	Temperature $T$ (°K)	Mach No. $M$	Velocity $V$ (meter/sec.)
0.2	0.043	76	3.81	664
0.4	0.112	99	3.14	629
0.6	0.197	116	2.76	602
0.8	0.295	131	2.51	575
1.0	0.409	145	2.30	551
1.2	0.524	155	2.14	532
1.4	0.645	164	2.00	516
1.6	0.782	173	1.88	498
1.8	0.929	181	1.77	482
2.0	1.078	189	1.67	465
2.2	1.225	197	1.58	447
2.4	1.398	205	1.50	428
2.6	1.552	212	1.42	412
2.8	1.730	218	1.35	397
3.0	1.883	224	1.28	382
3.2	2.065	230	1.21	366
3.4	2.26	236	1.14	350
3.6	2.44	241	1.08	334
3.8	2.63	246	1.02	319
4.0	2.80	250	0.96	306

TABLE III. Pressure, etc., as adiabatic functions of density (80-lb./in.<sup>2</sup> jet). (For equations used, see Table I.)  $C_p=1.00 \times 10^7$  erg/g °K;  $\rho_0=7.68$  mg/cm<sup>3</sup>;  $P_0=6.44$  atmos.;  $T_0=296^\circ\text{K}$ .

Density $\rho$ (mg/cm <sup>3</sup> )	Pressure $P$ (atmos.)	Temperature $T$ (°K)	Mach No. $M$	Velocity $V$ (meter/sec.)
0.2	0.04	68	4.08	675
0.3	0.07	80	3.66	657
0.4	0.10	90	3.37	642
0.6	0.18	106	2.98	616
0.8	0.27	119	2.71	595
1.0	0.37	130	2.51	576
1.2	0.48	140	2.35	558
1.4	0.59	149	2.21	542
1.6	0.71	157	2.09	527
1.8	0.84	165	1.98	512
2.0	0.97	172	1.89	498
2.2	1.11	179	1.80	484
2.4	1.26	185	1.72	471
2.6	1.41	191	1.65	458
2.8	1.56	197	1.58	445
3.0	1.72	202	1.52	434
4.0	2.58	227	1.23	371
5.0	3.52	249	0.97	306

method of characteristics the flow in a steady supersonic jet of air issuing at slightly supersonic speed from a circular orifice into a vacuum. Some results of this calculation, contained in Fig. 3.3 of their paper, are reproduced here in Fig. 15. This gives the pressure ratio  $p/p^*$  of the actual pressure at the axis of the jet, divided by the "critical pressure" as function of the ratio  $Z/D$ . The "critical pressure"  $p^*$  is the pressure of the gas when flowing at sonic speed, that is, for  $M=1$ ; it is connected with the "stagnation pressure" in the reservoir by the relation  $p^*=p_0[2/(\gamma+1)]^{\gamma/(\gamma-1)}=p_0 \cdot 0.528$  (if  $\gamma=1.40$ ).

The curve in Fig. 15 is taken from Owen and Thornhill's paper, the circles are the values obtained from our interferometric measurements for the axis ( $R/D=0$ , see Fig. 14), replacing  $p/p_0$  by  $p/p^*$  which is equal to  $p/p_0 \times 1.893$ . Such comparison is possible since the

values calculated for an infinite pressure ratio are universal values insofar as they are applied to any similar jet of cylindrical symmetry, if confined to an area bounded by the circular orifice and the first shock fronts. Also plotted as crosses are values of  $p/p^*$  as given in Fig. 3.3 of Owen and Thornhill's paper and taken from the paper by Hartmann and Lazarus (reference 8); they are obtained by pitot measurements along the axis of a jet flowing through a 6-mm orifice from a tank at a pressure of 7 kg/cm<sup>2</sup>. The agreement between the calculated and the measured values is pretty good, the slight

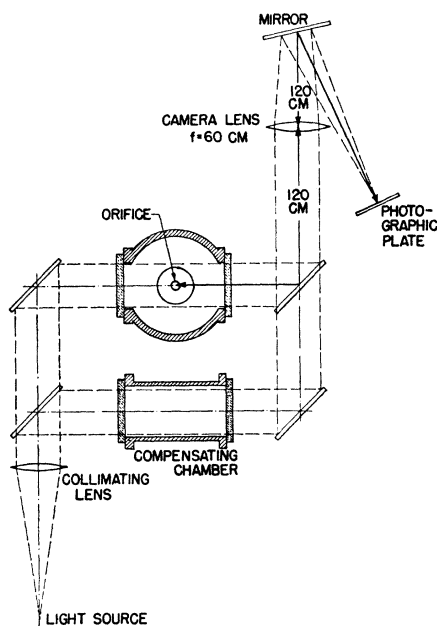


FIG. 8. Sketch of apparatus with vacuum chamber for studying jets at high expansion ratios by interferometry.

deviations, noticeable especially for small distances from the orifices, probably are due to the fact that the calculations start at a Mach angle of  $85^\circ$  ( $M = 1.004$ ) at the orifice; whereas, the Mach number at the orifice in the axis of our jets is approximately 1.05, that is somewhat higher than assumed in the calculations, so that the pressure ratios  $p/p^*$  are smaller than calculated. The calculations do not permit one of course—as was pointed out before—to determine the characteristic forms of shocks or for that matter the distance from the orifice where the normal shock is formed, since these features depend upon the pressure ratio  $p_0:p_{\text{outside}}$ , which was assumed in the calculations to be infinite.

### C. Prandtl-Meyer Flow at the Edges and the "Valley" Configuration

One prominent feature of the jets is the "valley" which appears in all isopycnic charts, extending up into the jet from the edge of the orifice (see Figs. 5, 6, and 7). This "valley" evidently marks the innermost region influenced by the outside atmosphere. We assume that

the expansion of the gas around the edge of the orifice, due to the overpressure in the jet, follows the Prandtl-Meyer type of flow, which very near the corner should be almost the same in the two- as in the three-dimensional case.<sup>h</sup> In the present case the pressure etc. of the air stream and the angular size of the Prandtl-Meyer expansion region, where the stream is turning outward from the orifice toward the atmosphere, depend on the form of the nozzle and the pressure in the reservoir. Assuming sonic velocity in the  $Z$  direction at the orifice, then one finds from the Prandtl-Meyer flow equations<sup>i</sup> that along a radius in the direction of the "valley" (dotted lines in Fig. 14) the pressure is less than the external atmospheric pressure. Some recompression, without visible shock waves, must occur between the "valley" and the outer jet boundary to build the jet pressure up to equality with the surroundings. The computed<sup>i</sup> short thin lines in Fig. 14, labeled 40, 60, etc., mark the atmospheric pressure point in the Prandtl-Meyer region. If the lines of constant ratio  $P/P_0$  (or  $\rho/\rho_0$ ) in Fig. 14 could be accurately determined near the orifice edge, they would directly map out the Prandtl-Meyer region, but the resolution of the experimental method does not permit this. The "valley" configuration does not appear to have been predicted from any of the theoretical jet studies so far. It can be approximately located by drawing the Mach line (see

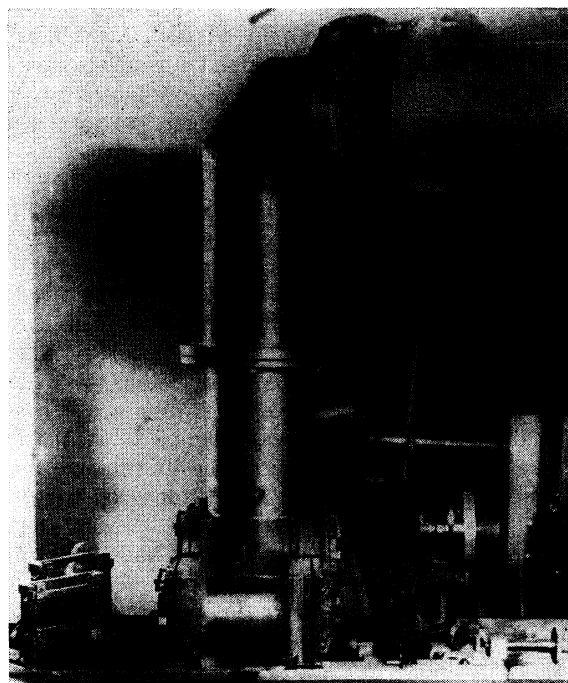


FIG. 9. Photograph of apparatus with vacuum chamber for studying jets at high expansion ratios by interferometry.

<sup>h</sup> See reference e, R. Sauer, p. 143. Also reference 18.

<sup>i</sup> Obtained by using the formulas on pp. 53-58 of R. Sauer's book and his Table II (see reference e).

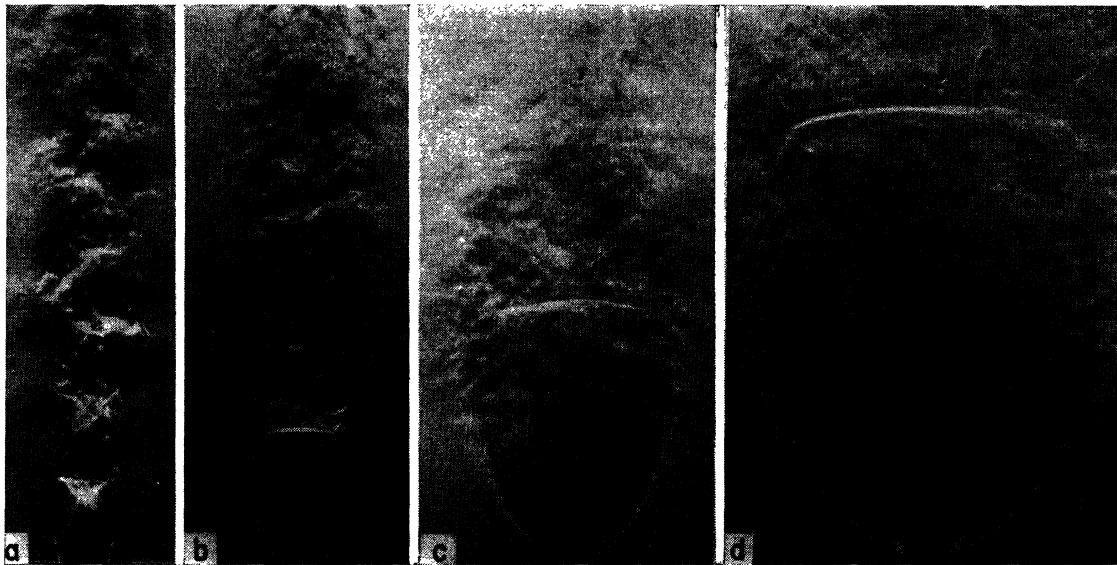


FIG. 10. Schlieren photographs at various expansion ratios, knife edge perpendicular to the flow. Expansion ratios: a, 5.1; b, 16.9; c, 57.5; d, 174.

III F) from near the orifice edge, which merges with the weak shock (herein designated shock 1) near the triple point.

**D. Shock Waves<sup>j</sup>**

The agreement between the measured normal shock strength  $\rho_2/\rho_1$ , where  $\rho_2$  and  $\rho_1$  are the densities on the downstream and upstream sides of the shock fronts, and the shock strength calculated from the Rankine-Hugoniot (R-H) relations,<sup>j</sup> is within the errors of the method, as shown in Fig. 13: there the dotted graph connects the values of  $\rho_2/\rho_0$  computed from the R-H relations for a normal shock in the form

$$\frac{\rho_2}{\rho_0} = \frac{\rho_1}{\rho_0} \left[ 1 - \left( \frac{\rho_1}{\rho_0} \right)^{\gamma-1} \right] \frac{\gamma+1}{\gamma-1}, \quad (1)$$

assuming  $\rho_1/\rho_0$  to be given by the smooth curve through all the experimental points. The normal shock appears clearly in the graphs for the 60-, 80- and 100-lb./in.<sup>2</sup> jets as a vertical rise of density reaching up to the dotted graph for  $\rho_2/\rho_0$  and confirms therefore the theoretical computations.<sup>k</sup> Small deviations from the R-H relations expected at large shock strength ( $\rho_2/\rho_1 > 3.5$ ) do not show up in our results since the accuracy of evaluation of axially symmetric jets is not sufficient.

Also the oblique shock strength has been compared with the R-H equations, with good success; for example, in the 60-lb./in.<sup>2</sup> jet, the calculated and observed shock strengths for shock 3 are 1.61 and 1.67, respectively.

<sup>j</sup> For literature on the theory of shock waves see reference e.

<sup>k</sup> The relatively larger deviation for the jet with only 4-mm orifice (60 lb.) may be due to the larger experimental uncertainty connected with the smaller diameter of the orifice.

**E. Mach Reflection**

It was pointed out in the introduction that the general shock-wave configuration characteristic of jets at the higher pressure ratios bears striking resemblance to the so-called "Mach" reflection of air shocks, first observed by E. Mach in 1878.<sup>12</sup> This phenomenon has been examined experimentally and theoretically in detail in recent years for the case of traveling air shocks with the result that the theory seems to be inadequate.<sup>15</sup> If one considers the oblique collision of a plane shock wave with a wall to be the same as the collision of this shock with its mirror image, one sees that a "simple" reflection at the wall (as in Fig. 16A) is possible over a certain range of strength and angles of the incident shock wave. Outside this range the "Mach" reflection appears, characterized by the point of reflection being away from the wall, and joined more or less normally to it by a third shock wave, as illustrated in Fig. 16B. The similarity between Fig. 16B and the air jets (Fig. 1B) is very great, but the development of the "triple shock" in the two cases may be quite different, as the jets are *stationary* phenomena and are axially symmetric. The Mach configuration, on the other hand, is a transient non-stationary phenomenon, enlarging continually as it moves along the wall, and cannot be brought to rest as a whole by a simple transformation to moving coordinates.

It must also be considered that the "core" of the jet after the normal shock wave is subsonic and therefore may transmit disturbances upstream to the shock region.

In spite of the differences between the triple-shock formation in the present stationary case and the shock formations in transient phenomena, it seemed worth

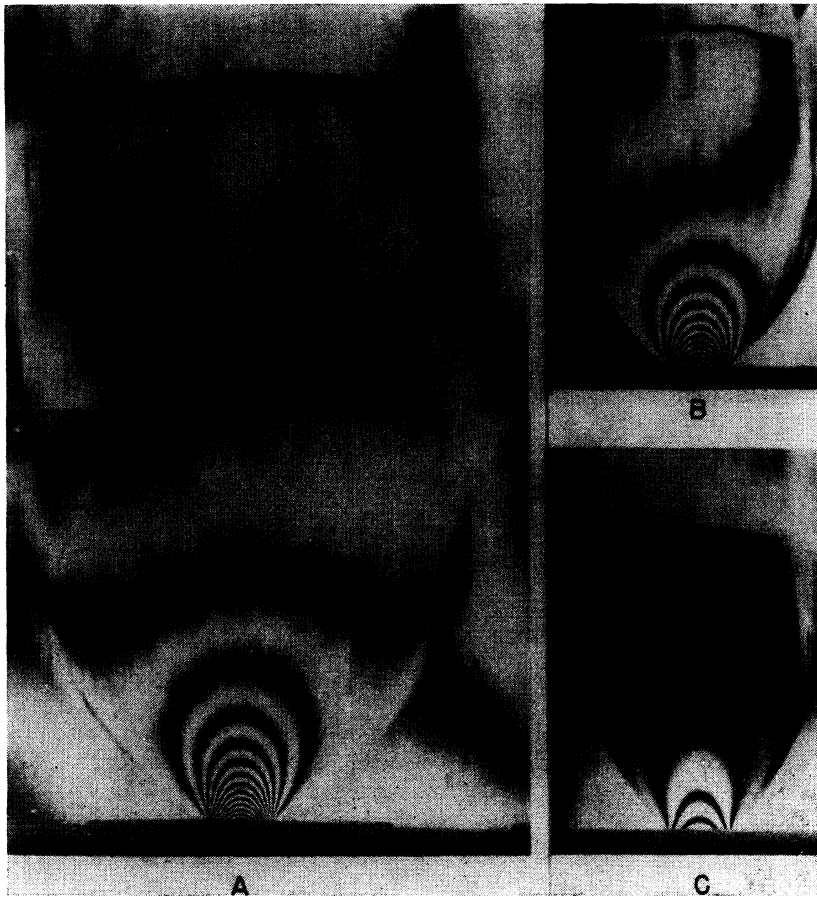


FIG. 11. Interferograms of axially symmetric air jets at high expansion ratios: A, 210; B and C, 60.

while to apply the theory of the triple-shock configuration<sup>15</sup> to the shock formation in jets, assuming that, although the present problem has axial symmetry in three dimensions, it may be considered as a two-dimensional case over a small region. However, preliminary computations have shown that neither the density values near the triple-point nor the shock angles could be measured accurately enough in this series of jets to provide a good check of the theory. For improving the accuracy and for simplifying the conditions, the homogeneous cylindrical jet escaping from a circular Laval nozzle at Mach number 1.7 has been studied as described in Paper I<sup>17</sup> using such tank pressures that triple shocks are formed in the open atmosphere. Figure 17 is an interferogram of a stationary triple shock under these conditions. The evaluation of such interferograms is not yet finished and shall be discussed in another paper.

#### F. Stream Lines and Mach Lines

A map of stream and Mach lines has been constructed in the case of the 60-lb./in.<sup>2</sup> jet by step-wise integration of the equations of motion, as described for the stream lines in a previous publication.<sup>17</sup> The Mach lines are constructed in an elementary, approximate way by

starting at various points along the axis which coincides with the flow direction. From the measured density at these points the Mach number and Mach angles are computed (as for one-dimensional flow) and so the Mach lines are drawn downstream as well as upstream as straight lines till they cross the next streamline and then the procedure is repeated. In this way Fig. 18 was obtained.

From the behavior of the stream and Mach lines near the orifice it can be concluded that the surface of  $M=1$ , which theoretically should coincide with the plane of the orifice, is curved back inside the edge, so

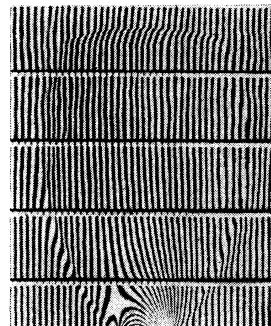


FIG. 12. Interferogram of an axially symmetric air jet at expansion ratio 60.

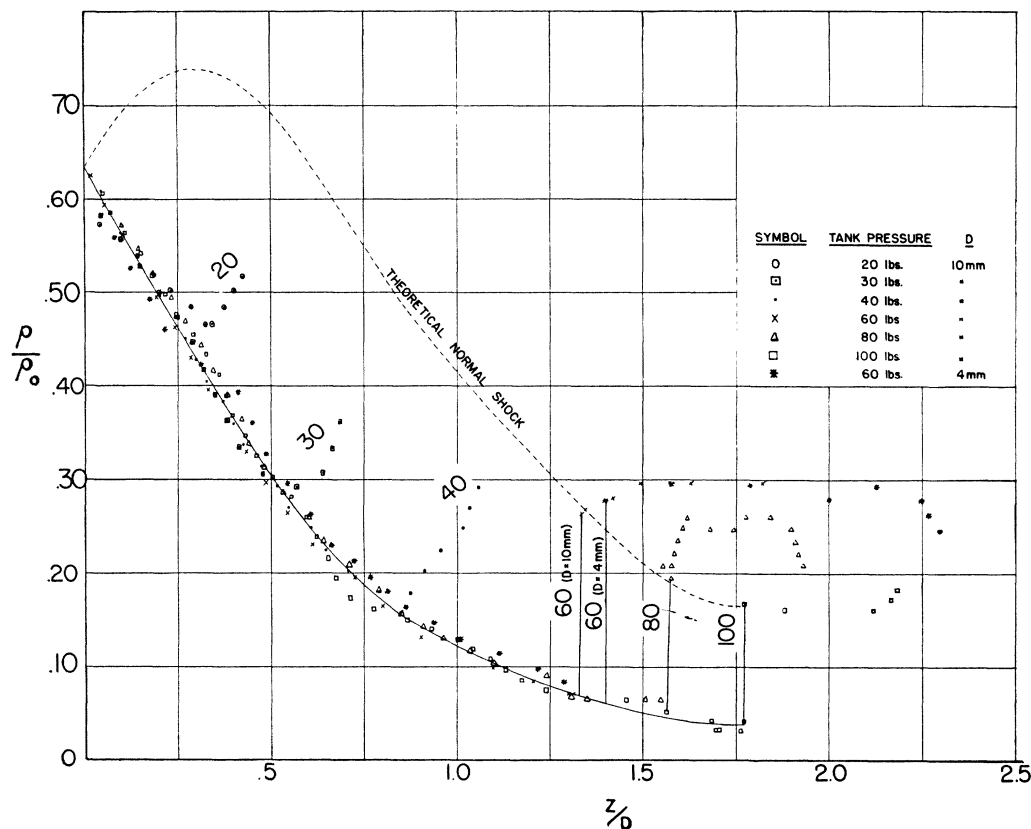


FIG. 13. The ratio  $\rho/\rho_0$  (density at fixed distance  $R$  from axis for various jets ÷ tank density) as a function of the ratio  $Z/D$  (distance from orifice ÷ orifice diameter) for  $R/D=0.1$ . The graph "Theoretical normal shock" connects the various values of  $\rho_2/\rho_0$  according to Eq. (1) section III-D.

that the air emerges near the edges with higher velocity, and immediately turns outward into the atmosphere. The negative Mach lines (the family with negative slope) diverging from the orifice edge show the three-dimensional Prandtl-Meyer region bounded by the "valley," which was shown in Fig. 14. The rate of expansion then decreases, the streamlines passing an inflection point at the "valley," and the jet reaches its maximum diameter at  $Z=8$  mm (Fig. 18). The "bottle" shape of the jet is easily understood, after one has constructed a few streamlines, to be the result of the interaction of the pressure and inertial forces of the out-streaming gas with the atmospheric pressure force to produce an overexpansion and then an overcontraction. This pattern is repeated at successive distances from the orifice, as shown in Mach's and Prandtl's pictures, also in some of the jets of our Fig. 1. However, the turbulence in these jets, which is rather conspicuous due to the short duration of the illuminating spark, destroys part of the repetition phenomena. They are most noticeable when the normal shock is not too large a part of the jet area, otherwise the transition to subsonic flow and corresponding loss of pressure head deteriorates the jet rapidly.

The negative Mach lines beyond the "valley" are

not expansion but compression waves due to reflexion at the boundary of the jet where it mixes with the outside air at rest (Fig. 18). When they converge, the pressure gradient steepens so that a shock is produced. This is the weak oblique shock 1 which forms well up in the jet towards the triple point. This shock appears on shadowgrams sometimes as a continuation of the "valley." In the case of jets at low pressure where shock 2 is absent, the "reflected" shock (Fig. 16) may be produced by interference of converging compression waves, which are due to reflexion of expansion waves at the other boundary between jet and air at rest. However, the appearance of the normal shock 2 at higher pressure and the subsonic core downstream from it cannot be understood from such elementary considerations (see Section III-E).<sup>1</sup>

#### IV. TWO-DIMENSIONAL JETS

The long and arduous reduction process which is inevitable in axial flows suggested the possibility of studying two-dimensional jets, analogous to the three-

<sup>1</sup> Similar conclusions are drawn by K. O. Friedrichs, App. Math. Group, New York University, AMG-NYU No. 47 (1944), from a series of unpublished shadowgrams of jets with various ratios and orifice shapes obtained by R. P. Fraser.

dimensional jets, but confined at all points between parallel glass walls. The density then is, in principle, constant along the light path and varies only in directions normal to this. The density at any point is given uniquely by the fringe shift at that point, independent of other points in the field. If the interferometer is adjusted for fringe contours (see Section II-B), all the

information is contained in the interferogram, the fringes of which may be labeled directly in terms of density, pressure, etc., without further measurement or evaluation. In two dimensions, as in three, some reference point of known density must be established in the field of view.

Interferometric investigations of two-dimensional

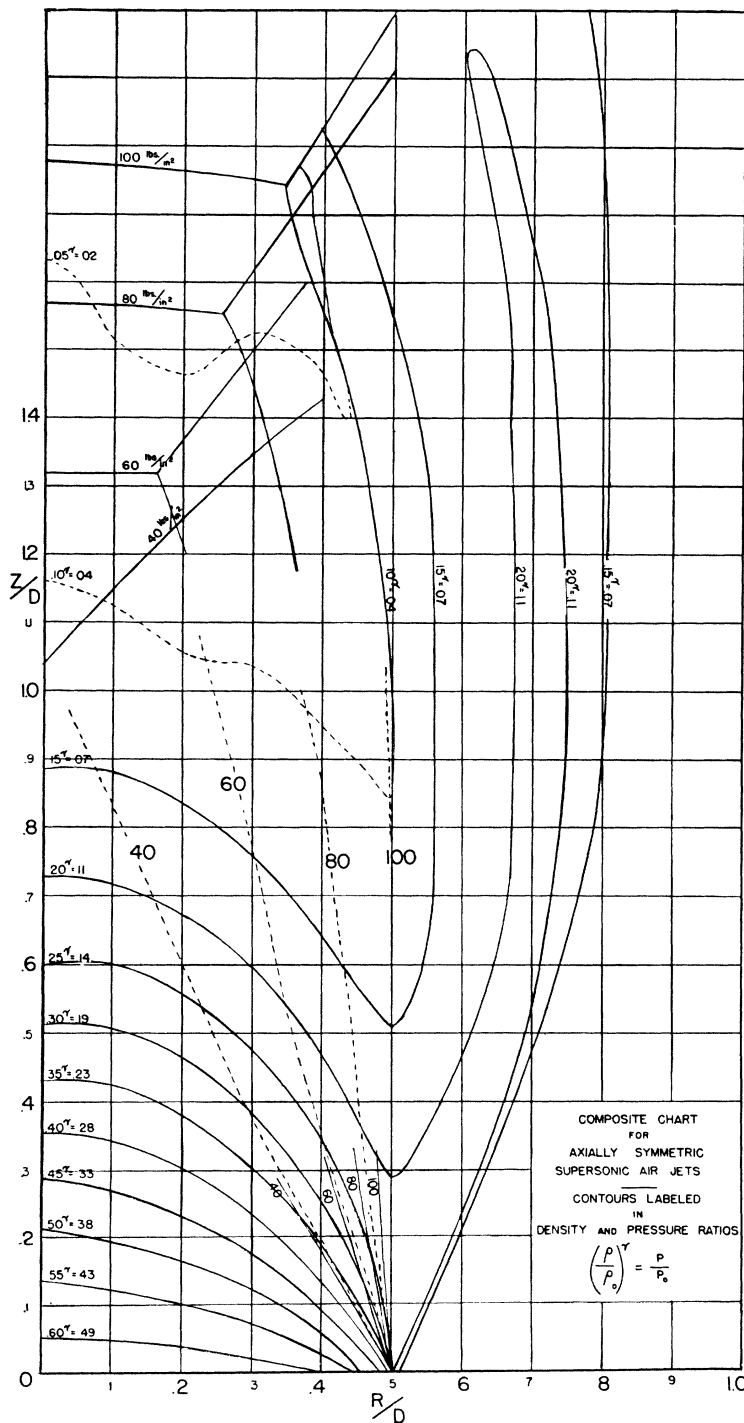


FIG. 14. Composite chart for jets at 40, 60, 80, and 100 lb./in.<sup>2</sup>. Contours labeled in density and pressure ratios  $((\rho/\rho_0)^\gamma = P/P_0)$ . The over-all figure is for the 100-lb./in.<sup>2</sup> jet, but it represents also the results of the jets at other pressures in a region bounded by the orifice, the shocks, and the "valleys" (the dotted lines).

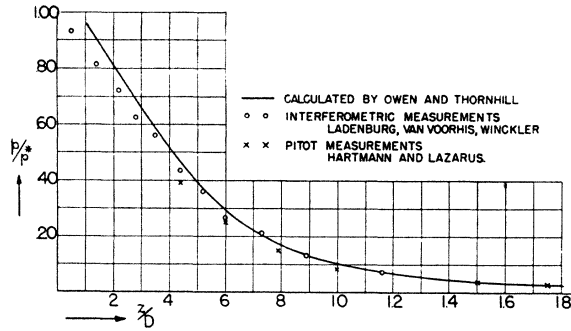


FIG. 15. Axial pressure distribution in supersonic jets as function of the ratio  $Z/D$  (distance from orifice divided by orifice diameter). Plotted is the ratio  $p/p^*$  of actual pressure divided by "critical pressure" which is the pressure of the gas when flowing at sonic speed.

flow, as in standard wind tunnels, permits also the study of a large number of additional phenomena—as, for example, boundary layers and their interaction with shock waves—which are not accessible in axially symmetric jets.

**A. Apparatus**

A two-dimensional nozzle was constructed, joined to the 1-in.-diameter round tube from the valve by a transition section. The nozzle consisted of two carefully ground and polished steel blocks, 20 mm in thickness along the light path. The nozzle contracted from the end of the 25-mm wide transition section down to the 4-mm orifice, and the blocks were then terminated. A 38-mm-wide region extended upwards from the orifice, which provided space for the jet to expand sideways. The glass plates were held firmly against the nozzle blocks. The air stream finally discharged into the 4-in. tube leading to the vacuum tank. The flow was kept between the glass plates, with a constant depth along the light path of 20 mm, and could expand only in directions normal to the light beam. A chamber with the compensating glass plates was inserted in the other light beam to equalize the optical paths as in the axially symmetric experiments. The exact shape of the nozzle may be seen in the interferogram, (Fig. 20) and as in the axially symmetric case the nozzle could be raised or lowered to bring various sections of the jet into the interferometer field of view.

**B. Experimental Results**

An interferogram made by the method of fringe contours of a two-dimensional jet expanding into a partial vacuum is shown in Fig. 19. The jet was found to be unstable, however, apparently due to the tendency of the air stream to exhaust partially the space between the glass windows and side walls into which it expanded, by sweeping air out. The jet would sometimes cling to a side wall or suddenly enlarge and fill nearly the entire space. An example of the latter behavior is given in

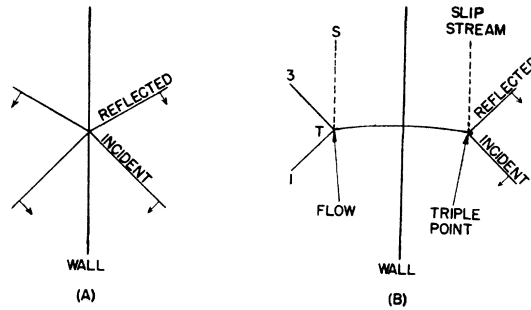


FIG. 16. Schematic drawing (A) of simple reflection and (B) of "Mach" reflection of a shock wave by a wall.

Fig. 20, which is obtained at the same tank pressure as Fig. 19 but at somewhat lower pressure in the vacuum tank. Figure 20 is a composite view of two sections of

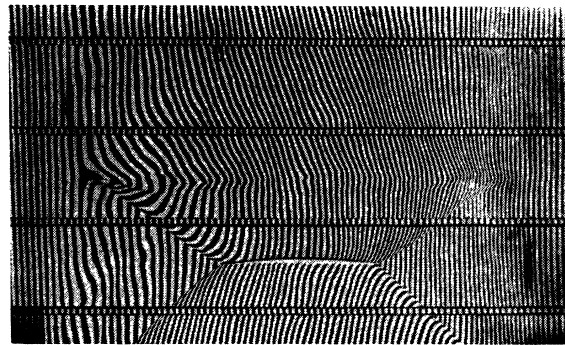


FIG. 17. Interferogram of a stationary "triple-shock configuration" in a homogeneous air jet leaving the orifice of the De Laval nozzle at about one atmosphere with Mach No. = 1.7.

the nozzle. Certain of the fringes have been labeled with their density value in  $\text{mg}/\text{cm}^3$ . From the relations

$$\left. \begin{aligned} \Delta s &= \Delta n d / \lambda, \\ \Delta n &= K \Delta \rho \end{aligned} \right\} \quad (2)$$

where  $\Delta s$  is the number of fringes counted,  $\Delta n$  the corresponding change of refractive index,  $d$  the length of light path (2.0 cm),  $\lambda$  the light wave-length ( $4.48 \cdot 10^{-5}$  cm),  $\Delta \rho$  the density change and  $K$  the Gladstone-Dale factor (0.228), one finds the density increment between adjacent fringes (black to black or white to white) to be  $0.103 \text{ mg}/\text{cm}^3$ . The reference point is taken to be the white fringe at the bottom of the photograph, at which point the pressure was measured with a fine hole in the side wall leading to a gauge. The density here is  $3.67 \text{ mg}/\text{cm}^3$ , calculated from the tank density and pressure, and assuming an adiabatic expansion to that point.

Theoretically, sonic velocity should be reached at a density of  $2.34 \text{ mg}/\text{cm}^3$  at the throat, and in actuality this occurs very close to the orifice for both Figs. 19 and 20. The density contours there are curves rather

than straight lines across the channel, indicating some departure from uniform conditions. This behavior is analogous to that of the axially symmetric jet, and stems from the section approaching the throat, which probably contracts too rapidly.

A well-defined "valley" extends downstream from the orifice edge, and in Fig. 20 what appears to be a normal shock wave exists in a manner somewhat like

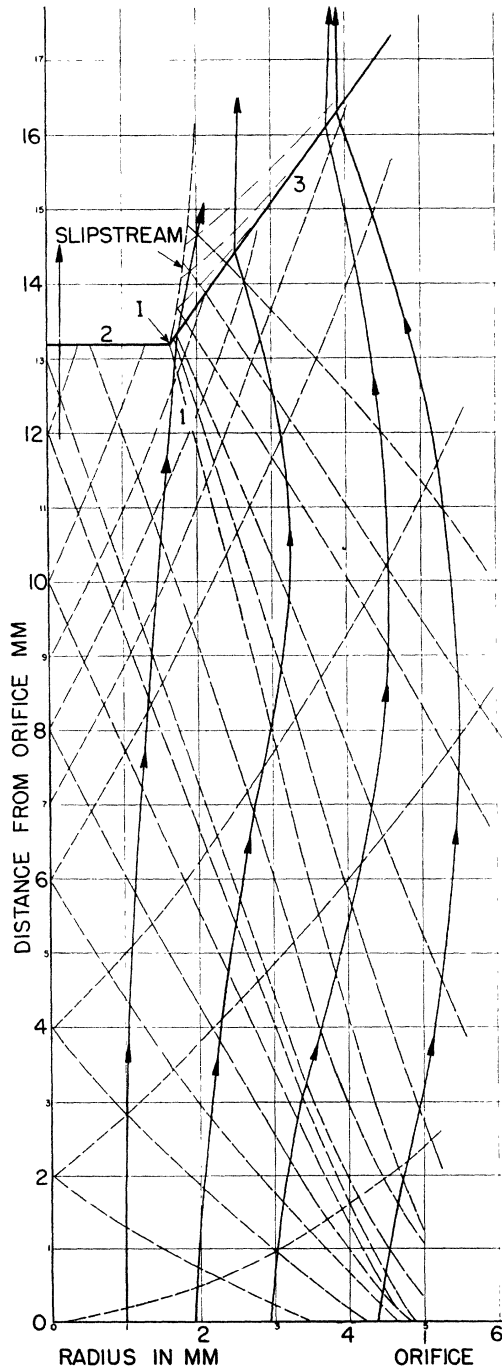


FIG. 18. Chart of computed stream lines and Mach lines for 60-lb./in.<sup>2</sup> jet.

the axially symmetric case, except that shock 1 is absent. From the density  $\rho_1=0.42$  mg/cm<sup>3</sup> just before this normal shock, we find from Eq. (1) that theoretically  $\rho_2=1.47$  mg/cm<sup>3</sup>. This corresponds to a fringe shift across the shock front of 10 units, although a close scrutiny of Fig. 20 shows a shift there of only about  $\frac{1}{2}$  unit.

This discrepancy is not due to an appreciable error in  $\rho_1$ , since this value has the correct ratio to  $\rho_0$  as computed from the ratio of the cross-sectional areas of the jet near the shock and at the orifice, according to the equation

$$(A/A_0)^2 = \frac{(2/(\gamma+1))^{\gamma+1/\gamma-1} \cdot (\rho_0/\rho_1)^{\gamma+1}}{2[(\rho_0/\rho_1)^{\gamma-1} - 1]/(\gamma-1)} \quad (3)$$

But the discrepancy between the observed and calculated fringe shift can be understood if the normal shock does not extend completely along the light path between the glass walls, but exists for only a small fraction of it. A reasonable explanation is that the boundary layer, inevitably present on the glass, is separated and enlarged by the pressure gradients of the normal shock, and produces a configuration of oblique shocks which destroys the two-dimensional quality of the flow. This separation phenomenon, if present, makes the observation of stationary shock wave patterns very difficult, as there is an unknown variation of density along the light beam. In fact, because of boundary layer separation, it is probable that the *stationary* Mach reflection in two dimensions is an experimental impossibility, and that one cannot produce in this way a stationary two-dimensional jet analogous to the axially symmetrical, three-dimensional jet.

### C. Two-Dimensional Flow in Channels (Experiments carried out by D. Bershader)

In order to avoid the instability of the jet, the latter was discharged not into an evacuated space, but into the atmospheric air after leaving the orifice, and it remained confined by the glass walls in the direction of the optical path. Two different nozzles have been constructed for these experiments; one was a "divergent channel," where the supersonic section was bounded by two plane steel walls, each making an angle of 4° with the axial plane of symmetry, essentially identical with a channel used 40 years ago by Magin in Prandtl's laboratory.<sup>7</sup> The other nozzle was constructed according to the "method of characteristics" in such a way that the supersonic velocity of the gas finally becomes uniform across the entire section. After leaving the correspondingly formed steel walls, the gas stream enters the atmospheric air, but remains between the glass walls. If the overpressure in the reservoir is such that the gas pressure at the orifice is near to atmospheric pressure, the gas stream does not expand sidewise, but



FIG. 19. Interferogram of contour fringes for two-dimensional jet, expansion ratio 6.1:1.



FIG. 20. Interferogram of contour fringes for two-dimensional jet flowing upward from reservoir through nozzle, fringes labeled in  $\text{mg}/\text{cm}^3$ . Expansion ratio 9.7:1.

proceeds with nearly the velocity it had reached in the uniform part of the channel.

The details of the experiments carried out with these two channels are reported in the thesis of D. Bershader and are published elsewhere.<sup>20</sup>

Only a few of his results which have a bearing on our foregoing conclusions will be mentioned here: the interferometric pictures of those jets show clearly the effect of the boundary layers along the walls of the channel and between the jet and the quiet air; the fringes, being straight in the main part of the channel, bend suddenly when approaching the edge of the jet, and crowd together; their evaluation permits the quantitative computation of the decrease of density and increase of temperature in the boundary layer and of its velocity profile. Furthermore, by rotating the channel through  $90^\circ$  and taking an interferogram of the light traveling

parallel to the glass walls above the orifice, one obtains also the effect of the boundary layer along the glass walls. Except for this boundary layer, the conditions are quite uniform from glass to glass up to a few millimeters above the orifice. However, farther out the pictures show clearly that the boundary layer against the glass begins to separate, destroying the homogeneity in the direction of the light beam, as was concluded before in discussing Fig. 20. The cause of this separation are the oblique shocks, which start at the orifice, and which evidently affect the boundary layer by their pressure gradient.

Our best thanks are due to Dr. H. Panofsky and Miss A. Kenny for very valuable help in carrying out this project.

<sup>20</sup> D. Bershader, *Rev. Sci. Inst.* **20**, 260 (1949); see further R. Ladenburg, *Proc. VII Int. Congress App. Mech.* London (in print).

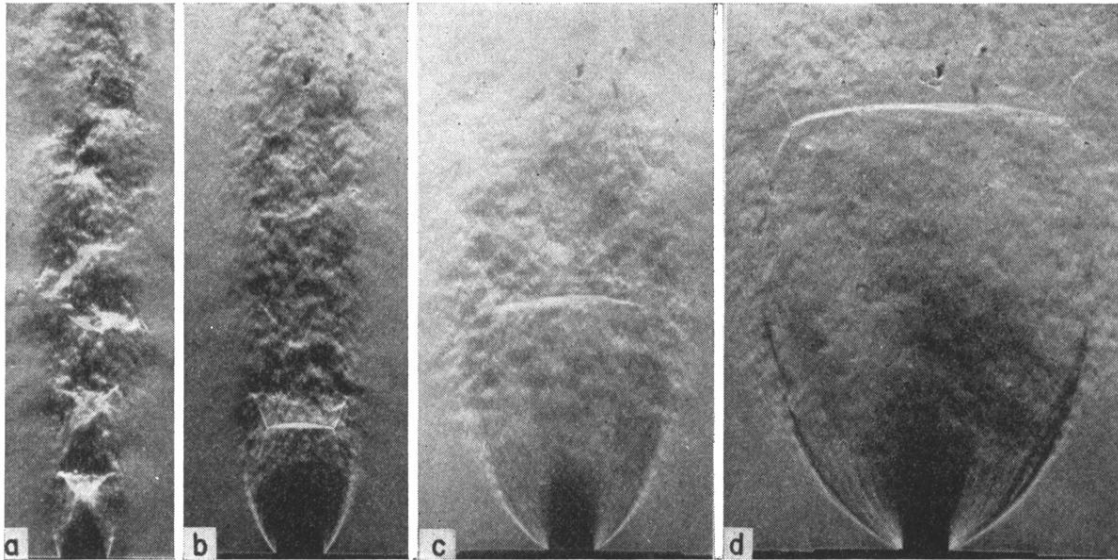


FIG. 10. Schlieren photographs at various expansion ratios, knife edge perpendicular to the flow.  
Expansion ratios: *a*, 5.1; *b*, 16.9; *c*, 57.5; *d*, 174.

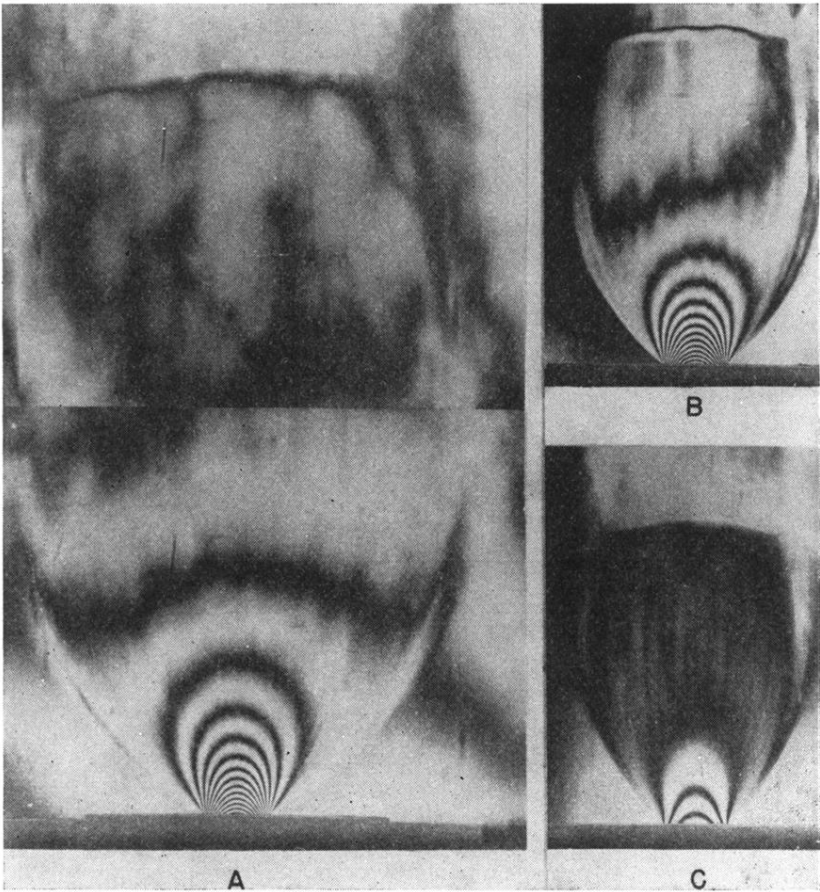


FIG. 11. Interferograms of axially symmetric air jets at high expansion ratios: A, 210; B and C, 60.

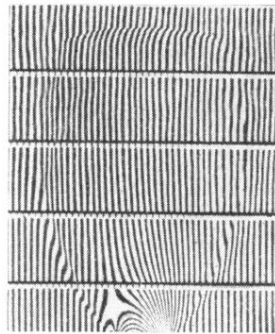


FIG. 12. Interferogram of an axially symmetric air jet at expansion ratio 60.

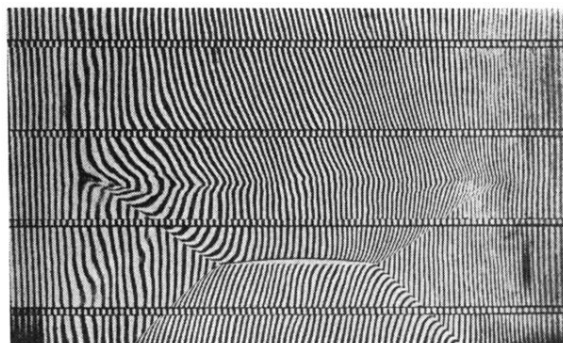


FIG. 17. Interferogram of a stationary "triple-shock configuration" in a homogeneous air jet leaving the orifice of the De Laval nozzle at about one atmosphere with Mach No. = 1.7.

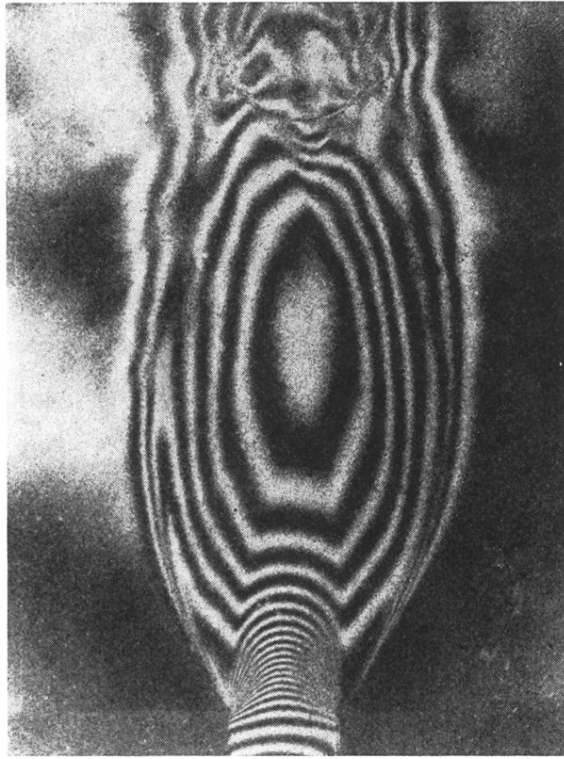


FIG. 19. Interferogram of contour fringes for two-dimensional jet, expansion ratio 6.1:1.

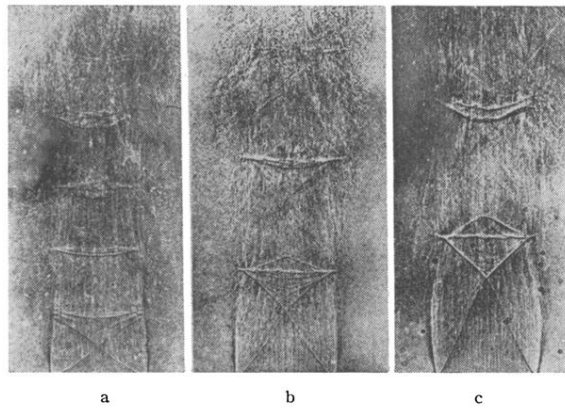


FIG. 1A. Shadowgrams of axially symmetric air jets flowing upward from a round orifice of 10-mm diameter. The black lines are generally the outlines of standing shock wave formations. The tank gauge pressure in a, b, and c are 20, 30, and 40 lb./in.<sup>2</sup>, respectively.

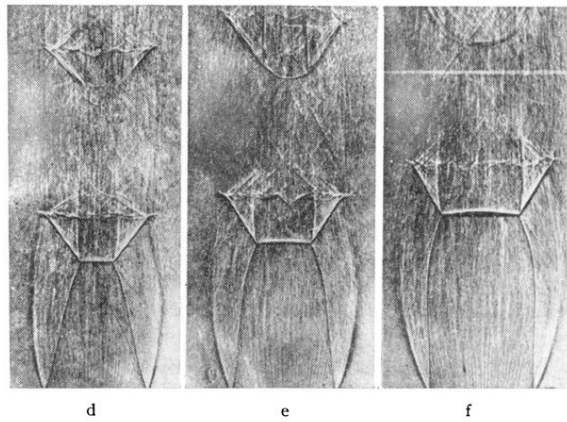


FIG. 1B. Shadowgrams as in Fig. 1A, the tank gauge pressures in d, e, and f are 60, 80, and 110 lb./in.<sup>2</sup>, respectively.

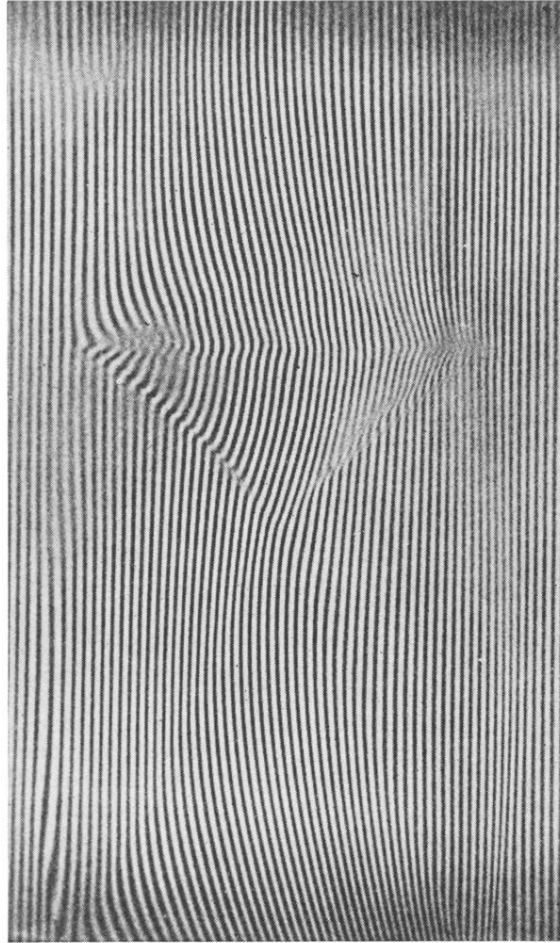


FIG. 2. Interferogram of an air jet issuing upward from a tank at 40-lb./in.<sup>2</sup> gauge through a 10-mm-diameter round orifice. (Compare with the shadowgram *c* of Fig. 1A.) The exposure ( $\sim 300 \mu\text{sec.}$ ) was too long to show turbulence.

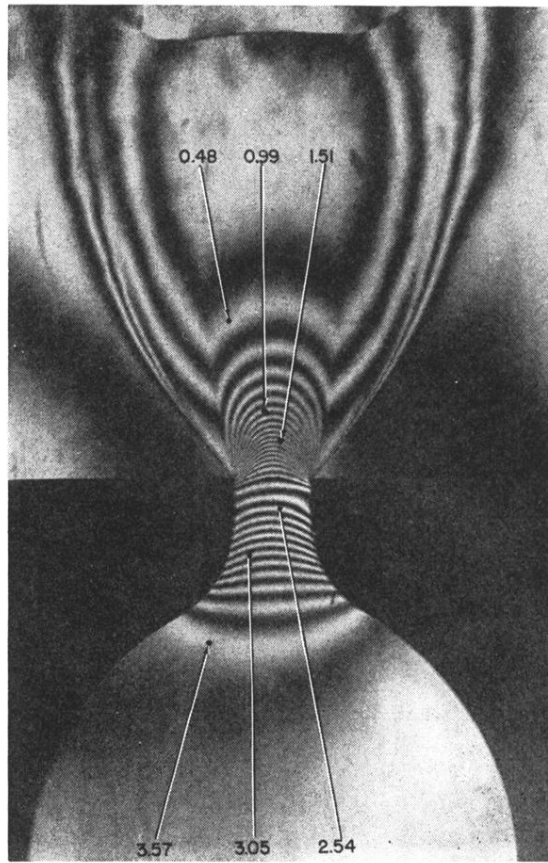


FIG. 20. Interferogram of contour fringes for two-dimensional jet flowing upward from reservoir through nozzle, fringes labeled in  $\text{mg}/\text{cm}^3$ . Expansion ratio 9.7:1.

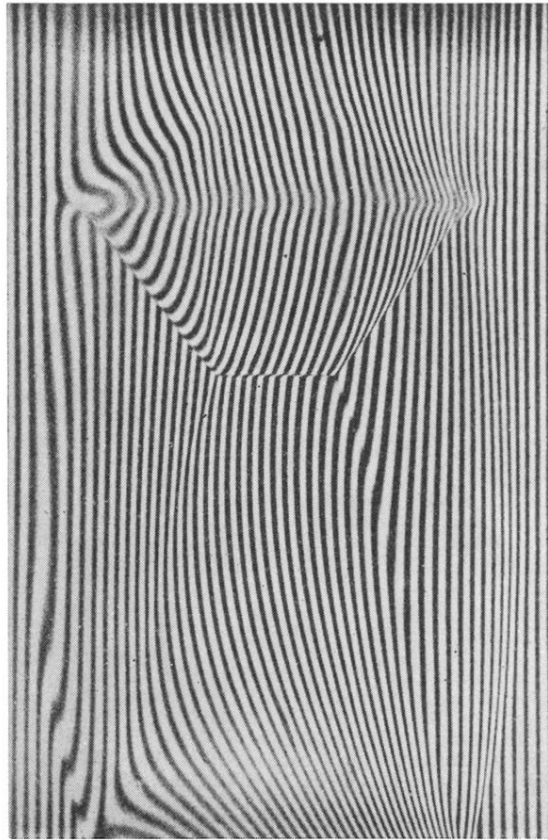


FIG. 3. Interferogram of an air jet at 60-lb./in.<sup>2</sup> gauge tank pressure (compare with shadowgram *d* of Fig. 1B). Exposure  $\sim 300 \mu\text{sec}$ .

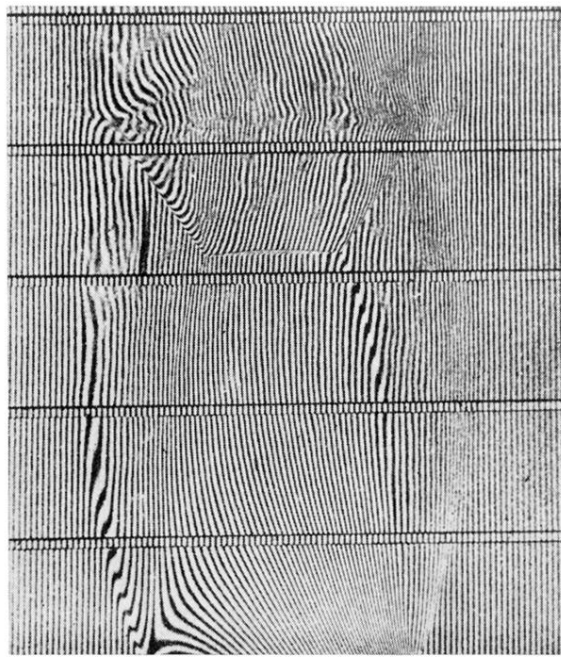


FIG. 4. Interferogram of an air jet at 80-lb./in.<sup>2</sup> gauge tank pressure (compare with shadowgram *e* of Fig. 1A.) Undisplaced fringes are superimposed in the narrow bands by means of grids. Note the turbulence, probably in the jet boundary, shown by irregularities in the fringes. Exposure 1  $\mu$ sec.

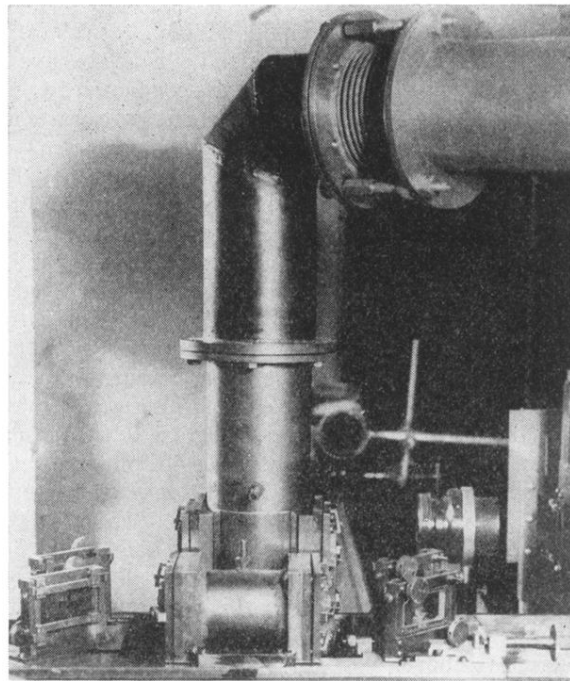


FIG. 9. Photograph of apparatus with vacuum chamber for studying jets at high expansion ratios by interferometry.